# Cadmium precipitation by sulfite reaction chain under UV irradiation

Tayebeh Rasolevandi[a], Hossein Azarpira[b], Amir Hossein Mahvi[a,c],*

[a]*School of Public Health, Tehran University of Medical Sciences, Tehran, Iran, emails: ahmahvi@yahoo.com/ahmahvi95@gmail.com (A.H. Mahvi), tayebe_r66@yahoo.com (T. Rasolevandi)*
[b]*Department of Environmental Health Engineering, Social Determinants of Health Research Center, Saveh University of Medical Sciences, Saveh, Iran, email: hazarpira912@gmail.com*
[c]*Center for Solid Waste Research (CSWR), Institute for Environmental Research (IER), Tehran University of Medical Sciences, Tehran, Iran*

**ABSTRACT**

Heavy metals in groundwater are potentially concerned because of their persistent toxicity, transformation to more toxic compounds, possibility of condensation, entry into the food chain. In this study removal of cadmium based on complexion in a UV/sulfite, and adsorption into $MnO_2$ was investigated. Herein, cadmium was removed completely in the optimal condition $Na_2SO_3$ = 0.3 mM, about 20 min reaction time (synthetic sample), pH 6, and 50 mg $L^{-1}$. Afterwards, the real sample was examined and anions increased with time to reach the standard from 20 to 30 min. In the first stage, the sulfite–sulfate cycle and reaction with cadmium and then both substances were removed from the solution by forming a complex. Advantage of this method against others includes less time, higher efficiency, less use of reactive materials, and removal of both Cd and sulfite. The amount of energy consumed decreased from 17.73 to 4.37 kWh $m^{-3}$, $K_{obs}$ ($min^{-1}$) 0.0915 to 0.1734 and $r_{obs}$ (mg $L^{-1}$ $min^{-1}$) increased from 3.57 to 43.35 with an increase in Cd concentration from 50 to 250 mg $L^{-1}$. Presence of anions, such as nitrate and sulfate, increased the cadmium removal efficacy. Nitrate reacted with $e^-_{aq}$ and with sulfite radicals and did not allow the formation of complexes; meanwhile, cadmium banding with sulfate helped its direct removal.

*Keywords:* Cadmium; Concern; Reduction; Radicals; Precipitation; Real sample

## 1. Introduction

Cadmium is a soft white silver metal chemically similar to the two stable metals zinc and mercury in Group 12 of the periodic table [1–3]. Cadmium, lead, mercury, and chromium are heavy metals without any physiological functions often considered to be toxic substances [4]. In areas with contaminated soil, water is a potential route for cadmium exposure [5,6]. Human resources of cadmium release into the environment, including copper and nickel smelting and refining industries, fossil fuel usage, electronics recycling [7]. According to the US Geological Survey, global cadmium productio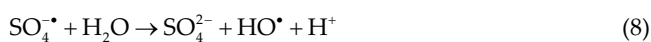n from 2017 to 2020 was approximately 23,000 tons [8]. Once cadmium enters the body, it travels in the bloodstream through red blood cells and albumin and then accumulates in the kidneys. Cadmium has been identified as a potential risk factor for cardiovascular diseases (CVD) [9,10]. In addition to the effects of cytotoxicity leading to apoptosis or necrosis, cadmium is a carcinogen for humans (Group I of the International Agency for Research on Cancer Classification) [11]. According to the US Environmental Protection Agency (EPA) guidelines, the maximum cadmium contamination in drinking water is 5 ppb due to these hazards [12]. Various methods, including chemical precipitation [13], adsorption or ion exchange such as ZIF-67/$Fe_3O4$ [14–16], polymer imprinted [4,17,18], electrochemical

treatment [2,19,20], advanced treatment processes (ATPs) [21,22], membrane technologies [23], and ozonation/UVA [24], for decontamination, separation of targeting contaminate from water and soils have been proposed. Advanced treatment processes (ATP) are able to achieve degradation (removal) of specific organic and inorganic ingredients in solution, which are not normally achieved through other treatment options [25]. Recent advances have highlighted advanced oxidation reduction processes (AORP) as possible options [26]. Inorganic anions, such as iodide, sulfite, carboxylate, or ferrocyanide, are stimulated to produce electrons and reduce species when exposed to a persistent UV activator [27–29]. To produce large amounts of electrons ($e_{aq}^{\bullet-}$), two properties are very important: UV absorption and electron production per absorbed photon, which in sulfite are 253.7 nm ($\varepsilon_{i}$, 254 = 220 M$^{-1}$ cm$^{-1}$, respectively) and $e_{aq}^{\bullet-}$ (e.g., 0.286 mol E$^{-1}$) [30]. In this paper, sulfite was used owing to its good properties. According to Eqs. (1)–(4), it produces electrons and reduces species:

$$SO_3^{2-} + h\upsilon \rightarrow SO_3^{\bullet-} + e_{aq}^{\bullet-} \tag{1}$$

$$HSO_3^- + e_{aq}^{\bullet-} \rightarrow H^{\bullet} + SO_3^{\bullet-} \tag{2}$$

$$H^{\bullet} + H_2O \rightarrow H_3O^+ + e_{aq}^- \tag{3}$$

$$H^+ + e_{eq}^{\bullet-} \rightarrow H^{\bullet} \tag{4}$$

Radical chain reactions can also occur in medium reaction [31,32].

$$SO_3^{-\bullet} + O_2 \rightarrow SO_5^{-\bullet} \tag{5}$$

$$SO_3^{-\bullet} + H^+ \rightarrow HSO_3^- \tag{6}$$

$$SO_5^{-\bullet} + HSO_3^- \rightarrow SO_4^{2-} + SO_4^{-\bullet} + H^+ \tag{7}$$

$$SO_4^{-\bullet} + H_2O \rightarrow SO_4^{2-} + HO^{\bullet} + H^+ \tag{8}$$

$$HSO_3^- + HO^{\bullet} \rightarrow H_2O + SO_3^{-\bullet} \tag{9}$$

Hydrated electrons as very strong reducing agents ($E_0 = -2.9$) can react directly with oxygen and produce H$^{\bullet}$ UV. It is one of the most common activation methods which has been widely employed to produce oxidants to form various AORPs. It is true that UV$_{254}$ rays are not able to react directly with water, but they can stimulate sulfite and create regenerative species or react directly with pollutants. Therefore, in this work, UV rays were applied to stimulate sulfite and remove direct and indirect cadmium in a photo reactor.

## 2. Martial and methods

### 2.1. Chemicals

All the chemicals were obtained from reputable companies and double distilled water (DDW) was used during this work. Sodium sulfite (Na$_2$SO$_3$) was purchased from Sigma-Aldrich. Cadmium solution was prepared from sodium–cadmium solution from Merck Company. Cadmium working solutions were obtained with appropriate dilution of the existing solution.

### 2.2. Reactor configuration

A UV lamp (nominal power: 11 W; light intensity: 78 $\mu$W cm$^{-2}$) with a wavelength emission in the range $\lambda_{max}$ = 254 nm was utilized as UV irradiation source with quartz sleeve fixed in center of the tubular glass (distance of 1 cm from the quartz). Cadmium solution was entered in the empty space between the quartz and tubular glass as reaction space. The experiments were performed in a 500 mL container. To prevent the effect of the lamp temperature on the reaction and disturbance in the results obtained, water was rotated around tubular glass.

### 2.3. Analytical methods

In Cd photo-precipitation, the effects of initial Cd concentration (50–250 mg L$^{-1}$), initial pH (3–11), and photo-reaction time (0–120 min) were investigated. Graphite atomic absorption spectroscopy was employed to measure the residual cadmium concentration. The following equation was applied to determine the photo-precipitation of Cd.

$$Cadmium\ photo-precipitation = \frac{Cd_0 - Cd_t}{Cd_0} \tag{10}$$

where Cd$_0$ and Cd$_t$ are defined as the Cd concentration (mg L$^{-1}$) at the beginning and during the time of the reaction, respectively. In addition, the effect of anions on the photo-precipitation of Cd was studied.

### 2.4. Kinetic model and energy consumption estimate

Since it is almost impossible to determine the amount of reducing species in solutions, according to Eqs. (11) and (12), the pseudo-first-order was used to study the Cd reduction model.

$$\ln \frac{C_t}{C_0} = -K_{obs}t \tag{11}$$

$$r_{obs} = -k_{obs}C \tag{12}$$

where $K$ is the constant coefficient of reaction rate.

Important factors, such as economy, wastewater quality, and cost, also play a key role in choosing a treatment technology. The major part of the cost of photo processes in the removal of water pollutants is related to electrical

energy. Although there are several methods on determining the AORPs electrical energy consumption in the literature and it depends on the type of pollutant, effluent quality, the reactor configuration, and the type of light source used, it is necessary to study the AORPs electrical energy consumption under experimental conditions. The International Union of Pure and Applied Chemistry (IUPAC) has introduced the parameter of energy consume for each order (figure-of-merit) briefly called $E_{EO}$ to determine the amount of electrical energy (kWh) in UV-based reactions. Electrical energy per order $E_{EO}$ allows to quickly determine the electrical energy consumption and shows the total energy required. For the purpose of comparison, the treatment efficiency for different processes was evaluated through $E_{EO}$ values. This means that the energy utilized almost 90% of photo-remove contaminants in 1 m$^3$ of contaminated water. The $E_{EO}$ values were obtained by inverting the slope of a log$C/C_o$ vs. UV dose [26].

$$\text{IUPAC } E_{EO} = \frac{P \times t \times 1,000}{V \times 60 \times \log \dfrac{C_i}{C_f}} \tag{13}$$

where $P$ is the amount of power (kW), $V$ is the volume (L), and $t$ is the photo-reaction time (min) of water in the photoreactor. By combining and rearranging Eqs. (11) and (13), a new $E_{EO}$ is obtained based on kinetic equation [33].

$$\text{Kinetic } E_{EO} = \frac{P \times 38.4}{V \times K_{obs}} \tag{14}$$

### 2.5. Reduction and oxidation species activity tests

The photocatalytic tests were carried out in UV-only, UV/sulfite, and dark condition (sulfite only), in percent of oxidative and reductive scavengers at the optimal condition. The initial concentration of Cd was 50, 100, and 250 mg L$^{-1}$. To understand the role of SO$_4^{\bullet-}$ and O$_2^{\bullet-}$ and reductive species in the mechanism of the Cd removal, experiments with the addition of oxidative and reductive species scavengers, including isopropyl alcohol, sodium oxalate, and benzoquinone and nitrate (10 mL scavengers in 100 mL of Cd aqueous solution) were conducted [34,35]. For all the tests, the reactor was in the dark for 1 h before the UV lamp was turned on. During the test, several samples were collected at constant times and the concentrations of Cd and were analyzed.

## 3. Result and discussion

### 3.1. Effect of pH

The effect of pH on Cd removal in dark, UV-only, and UV/sulfite (US) process were investigated over a wide pH range (3–11). As shown in Fig. 1, without irradiation, the removal of Cd at pH 3 was insignificant (about 20%) and then decreased with increasing pH. It can be concluded that the adsorption rate of cadmium by sulfate particles is 20%. The effect of the presence of sulfite revealed that Cd removal increased with decreasing pH. To explain this pH dependence, Cd removal was performed under light conditions at 5 different pH values (pH 3–11). In numerous studies, the rate of Cd oxidation increased with decreasing pH level, which is consistent with the findings of our study [36–38]. Photo reduction/removal of cadmium at pH 7 was studied by Nguyen et al. [39] using TiO$_2$ as the photocatalyst and with formate or methanol as the cavity controller (h$^+$) and in the absence of organic additives, about 60% of 30 ppm cadmium was removed from the solution. In a study by Salmanvandi et al. [40], The removal of cadmium (Cd(II)) ions applying a bentonite-supported Zn oxide (ZnO/BT) photocatalyst, the maximum reduction/removal efficiency of 74.8% was obtained at pH 5, contact time 6 h, 6 ppm Cd(II), and 4 g of ZnO/BT.
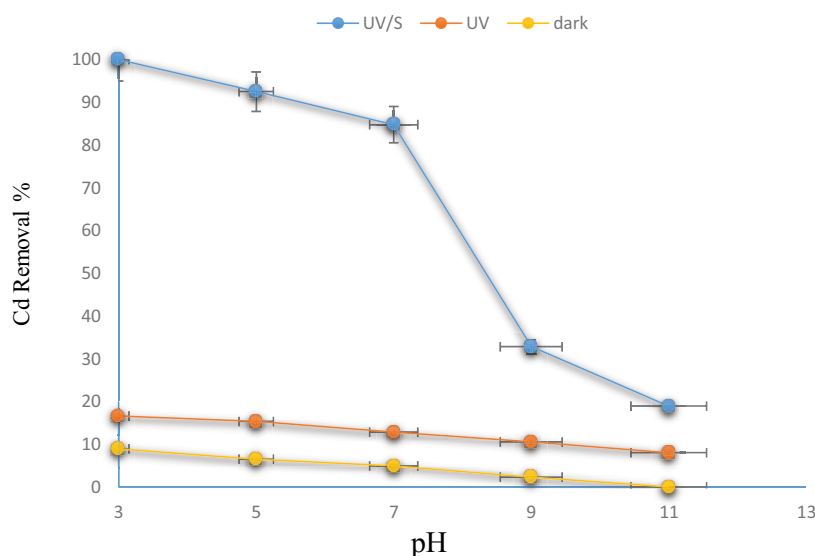


Fig. 1. Effect of pH on the removal of Cd (Experimental conditions: sulfite: 1 mM, Cd = 100 mg L$^{-1}$, 60 min reaction time).

*3.2. Reducing and oxidizer species activity tests in cadmium photo-precipitation*

To gain further insight into the reduction and oxidation mechanism in the UV/sulfite process, we investigated the quota of different species by scavengers at pH 6 and 8. As shown in Fig. 2, reducing species seem to be the predominant species. At pH 6, about 30% and 70% of reaction species were oxidative and reduction species, respectively. On the other hand, at pH 8 about 60% and 40% of the reaction species respectively were oxidative and reduction species. Inspection of Fig. 2 reveals that the contribution of reactive species at pH 6 with best performance to Cd removal are $SO_3^{\bullet-}$ and $SO_4^{\bullet-}$ radicals. At pH 8, a significant difference is observed probably due to the low percentage of soluble sulfite and the presence of sulfate radical ($SO_4^{\bullet-}$) with a high oxidation potential ($E_0 = 2.60$ V vs. NHE) in reaction medium at this pH. According to Fig. 3, the reaction rate of different processes demonstrates that the UV/S is very rapid process in Cd photo-precipitation. At pH 3, a significant difference was observed probably due to the low percentage of sulfate radical at this pH [41]. Since the performance of the system was better at pH 6, probably the sulfate–sulfite cycle was formed and the cadmium
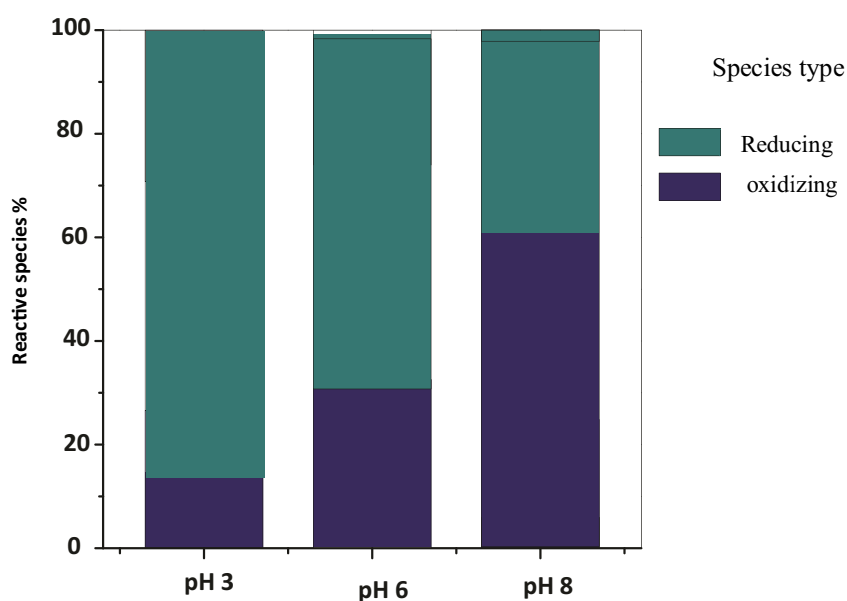


Fig. 2. Reducing and oxidizer species in cadmium photo-precipitation at various initial pH values (Experimental conditions: sulfite: 1 mM, Cd = 100 mg L$^{-1}$, 60 min reaction time).
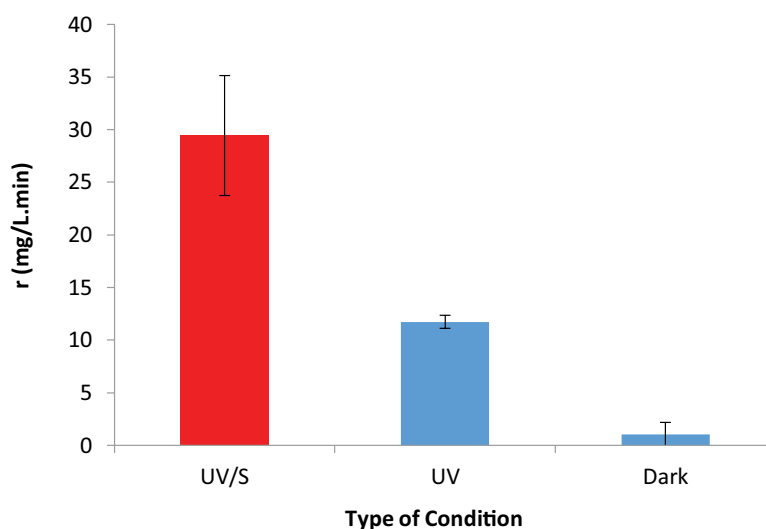


Fig. 3. Reaction rate of different conditions of cadmium photo-precipitation at various initial pH values. (Experimental conditions: sulfite: 1 mM, Cd = 100 mg L$^{-1}$, 60 min reaction time).

photo-precipitation strengthened. It also revealed that reducing agents play a more primary role in the reaction; however, oxidizers are also very important. In the presence of sulfite, $K_{obs}$ is significantly higher than that in the absence of sulfite over the whole investigated pH range [31].

### 3.3. Effect of different sulfite dose

Different amounts of sulfite were used to investigate the effect of sulfite dosage on Cd removal at pH 6 and fixed sulfate dose at 1 mM. Determined $C/C_o$ values were plotted against sulfite dosage in Fig. 4. $C/C_o$ values decreased initially with the increase in sulfite dosage, reached a maximum value at 0.3 mM, and then decreased. Sulfite can cause chain reactions producing sulfur oxy and $SO_3^{-\bullet}$ radicals and increasing the sulfite concentration can improve the initial oxidation rate. However, they can react with sulfite by over-increasing the produced radicals $SO_4^{-\bullet}$ and $SO_3^{-\bullet}$ when applied at much higher concentrations.

### 3.4. Kinetics and energy consumed in the photo-precipitation process

In cost-effective factors, energy consumption is a limiting factor in the use of AORP process. In the current study, kinetic and IUPAC methods were utilized to calculate photo-process energy consumption. The calculation of $R^2$ (0.97) in Table 1 indicates the fact that the cadmium photo-precipitation process follows the pseudo-first-order kinetics. The values of $R^2$ are given in Table 1 and are calculated according to Fig. 5. The reaction rate increased with raising concentration, which is due to the oxidizing

and reducing species colliding with cadmium and sediment formation. On account of the need for more time or insufficient generate of reactive species to the precipitation of cadmium in high concentrations, the reaction rate decreased at 100 mg L$^{-1}$ concentration. In kinetic and IUPAC methods, energy consumption has increased with increasing cadmium concentration and according to the formula it is clear that more cadmium precipitation at higher concentrations requires more energy. Moreover, the proximity of the energy obtained with the kinetic method in the range of energy obtained from the IUPAC method indicates the accuracy of the calculations. Constant reduction and reaction rate was probably due to a lower chance of cadmium colliding with reactive species or insufficient generation of reactive species to the sediment of high cadmium concentrations. It leads to a decrease in the efficiency of the precipitation process and the constant and reaction rate are therefore reduced [42]. The amount of consumed energy decreased from 17.73 to 4.37 kWh m$^{-3}$, $K_{obs}$ (min$^{-1}$) 0.0915 to 0.1734, and $r_{obs}$ (mg L$^{-1}$ min$^{-1}$) increased from 3.57 to 43.35 because the amount of consumed energy varies depending on the concentration of the pollutant. In many studies, energy consumption increases with increasing pollutants, but in several others it is quite the opposite and the amount of energy consumption decreases with increasing pollutant concentration [28,43].

Heavy metal such as Cd can react with $SO_3^{-\bullet}$ and $SO_4^{-\bullet}$ radicals in the aqueous medium [44], and then S-Cd can be react by the MnOOH$^\bullet$ and form a stable complex.

*Step 1*

$$SO_3^{2-} + h\upsilon \rightarrow SO_3^{\bullet-} + e_{aq}^{\bullet-} \tag{15}$$
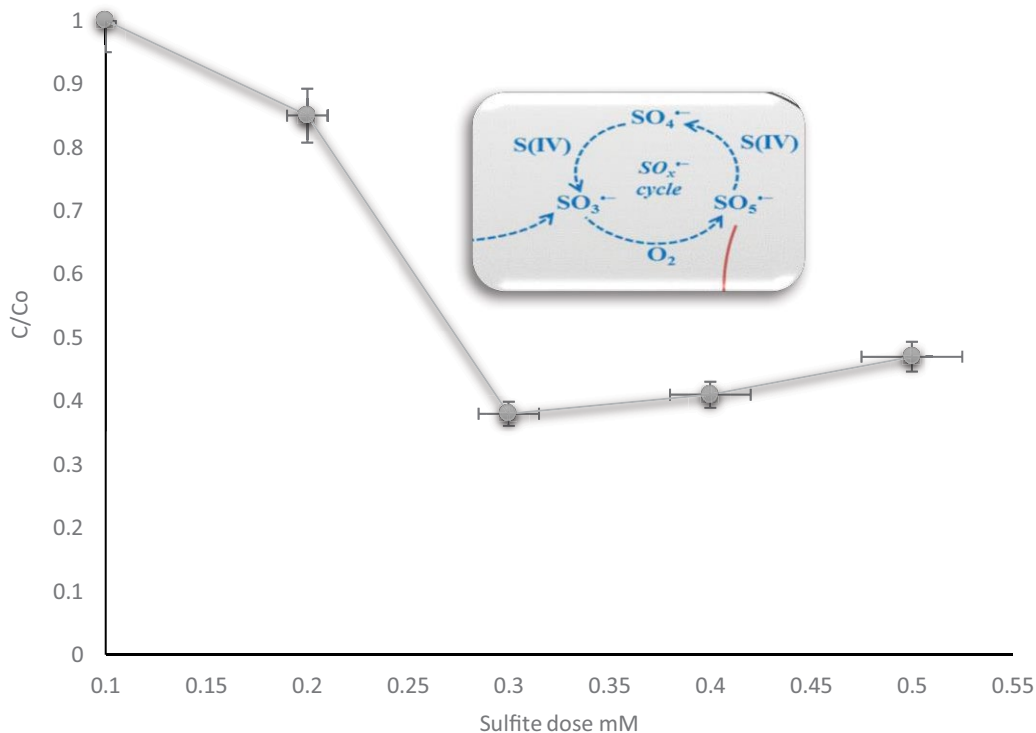


Fig. 4. Effect of sulfite dose on Cd removal (Conditions: pH: 6, Cd = 100 mg L$^{-1}$, 10 min reaction time).

Table 1
Pseudo-first-order kinetics and electrical energy used in different initial Cd concentration

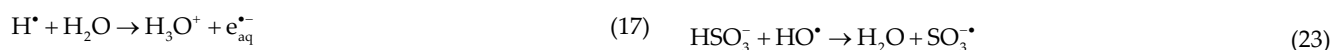| | | | Photodegradation pseudo-first-order | | |
|---|---|---|---|---|---|
| Cd (mg L$^{-1}$) | $R^2$ | $K_{obs}$ (min$^{-1}$) | $r_{obs}$ (mg L$^{-1}$ min$^{-1}$) | Kinetic $E_{EO}$ (kWh m$^{-3}$) | Figure-of-merit $E_{EO}$ (kWh m$^{-3}$) |
| 50 | 0.9582 | 0.0715 | 3.575 | 17.73 | 12.66–17.41 |
| 100 | 0.9692 | 0.1218 | 12.18 | 8.61 | 7.26–10.15 |
| 250 | 0.9852 | 0.1734 | 43.35 | 4.37 | 3.24–8.12 |
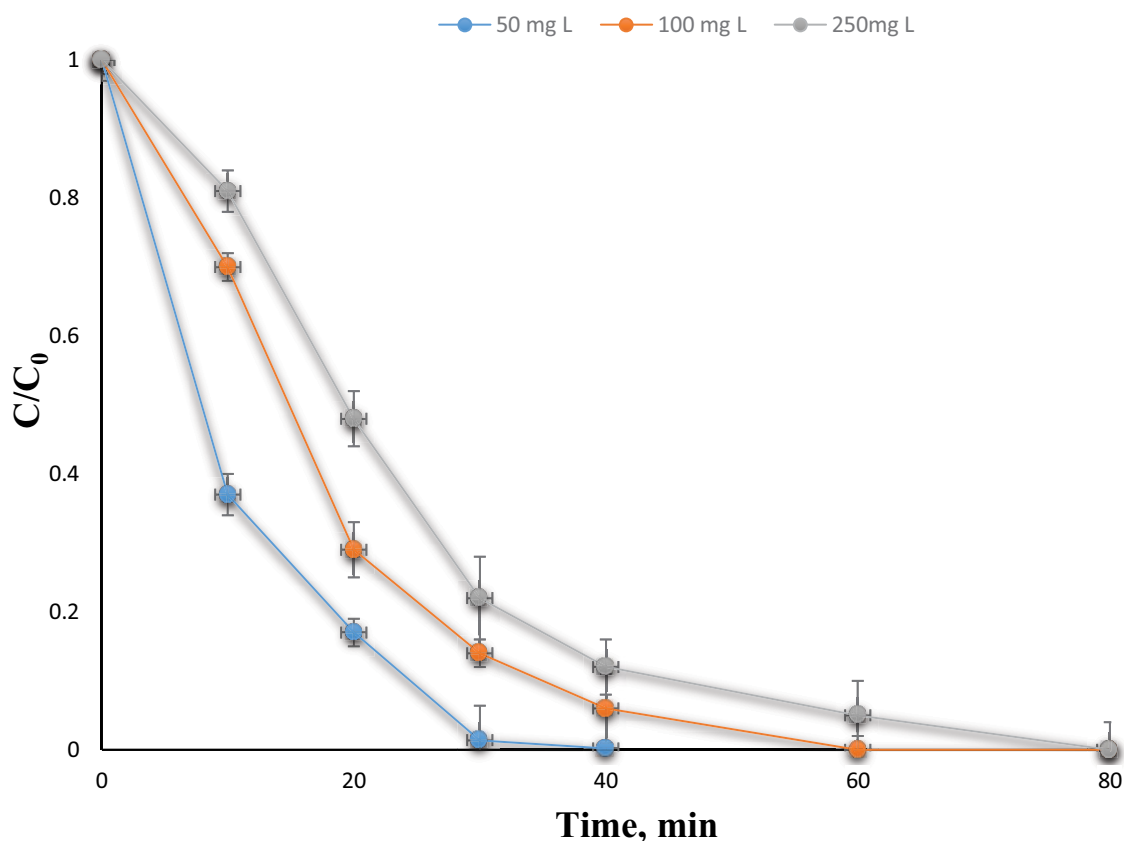


Fig. 5. $C_t/C_o$ vs. $t$ to calculate reaction rate constant (Conditions: [Na$_2$SO$_3$] = 0.3 mM, pH 6).

$$SO_3^{2-} + e_{aq}^{\bullet-} \rightarrow H^{\bullet} + SO_3^{\bullet-} \tag{16}$$

$$H^{\bullet} + H_2O \rightarrow H_3O^{+} + e_{aq}^{\bullet-} \tag{17}$$

$$H^{+} + e_{eq}^{\bullet-} \rightarrow H^{\bullet} \tag{18}$$

$$SO_3^{\bullet-} + O_2 \rightarrow SO_5^{-\bullet} \tag{19}$$

$$SO_3^{\bullet-} + H^{+} \rightarrow HSO_3^{-} \tag{20}$$

$$SO_5^{-\bullet} + HSO_3^{-} \rightarrow SO_4^{2-} + SO_4^{-\bullet} + H^{+} \tag{21}$$

$$SO_4^{-\bullet} + H_2O \rightarrow SO_4^{2-} + HO^{\bullet} + H^{+} \tag{22}$$

$$HSO_3^{-} + HO^{\bullet} \rightarrow H_2O + SO_3^{\bullet-} \tag{23}$$

$$Cd(NO_3)_2 + SO_3^{\bullet-} \rightarrow CdSO(S-Cd) \tag{24}$$
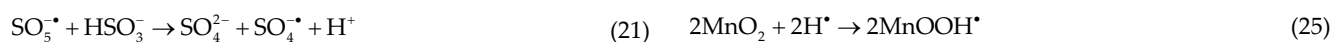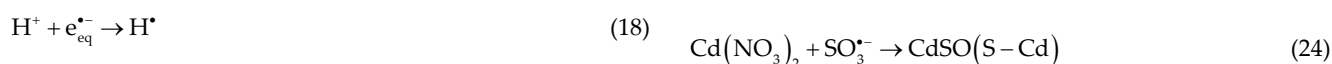
*Step* 2: Where MnOOH$^{\bullet}$ is a reactive hydroxyl group on the manganese oxide surface and the 2MnO$_2$·CdOOH is a surface complex. Also, radical chain reactions can occur in medium reaction [31,32].

$$2MnO_2 + 2H^{\bullet} \rightarrow 2MnOOH^{\bullet} \tag{25}$$

$$2MnOOH^\bullet + CdSO^- \rightarrow 2MnO_2 \cdot CdOOH \qquad (26)$$

$$SO_3^{-\bullet} + O_2 \rightarrow SO_5^{-\bullet} \qquad (27)$$

$$SO_3^{-\bullet} + H^+ \rightarrow HSO_3^- \qquad (28)$$

$$SO_5^{-\bullet} + HSO_3^- \rightarrow SO_4^{2-} + SO_4^{-\bullet} + H^+ \qquad (29)$$

$$SO_4^{-\bullet} + H_2O \rightarrow SO_4^{2-} + HO^\bullet + H^+ \qquad (30)$$

$$HSO_3^- + HO^\bullet \rightarrow H_2O + SO_3^{-\bullet} \qquad (31)$$

### 3.5. Precipitation of cadmium and sludge survey

The sludge survey is an important issue in Cd precipitation and to perform it, 1,000 ppm of cadmium solutions were tested. White sludge particles are exhibited in Fig. 6. Fourier-transform infrared spectroscopy (FTIR) analysis was employed to detect the type of sludge. As shown in Fig. 7, the broad band at 3,454 cm$^{-1}$ was observed in the spectra of all the samples related to Cd–S [45]. Furthermore, two peaks were observed in the FTIR spectra of Cd at 1,064 and 992 cm$^{-1}$ can be attributed to the –Cd–O band [46], respectively. This is supported by new a peak in FTIR spectrum of Cd-OH at 619 cm$^{-1}$, suggesting the formation of Cd(OH)$_3$ and a peak at 1,412 cm$^{-1}$, associated with the stable Cd$_2$O$_3$.

### 3.6. Impact of anion in real sample on Cd photo-precipitation

Common anions in water and wastewater interfere with AORPs and reduce their effectiveness. The amount of water ions may also change after AORPs processes, particularly photo-precipitation. To explore the US process application for the treatment of cadmium-contaminated water, the experiments in two water matrix, including distillated and underground water (real sample with Cd additive), were carried out and the results are presented in Fig. 8. Obviously, the US process effectively removed the cadmium from different water matrix and all the cadmium concentrations were reduced to a value of less than 100 mg L$^{-1}$ (the maximum permissible cadmium level) after 10 min of US process, suggesting the great potential of the US process on practical applications for cadmium removal. Fig. 8 illustrates that the examined ions increased the time to reach the standard from 20 to 30 min (100 mg L$^{-1}$) once the actual sample was applied. The presence of nitrate led to a decrease in removal regardless of the pH tested. CdNO$_3^-$ has an atomic structure similar to that of cadmium and can compete with Cd for adsorption onto permanganate formed and completely inhibit Cd removal [47]. In addition, to investigate the involvement of anions in photo-precipitation and the effect of photo-precipitation on the amount of anions before and after photo-precipitation, the amount of anions



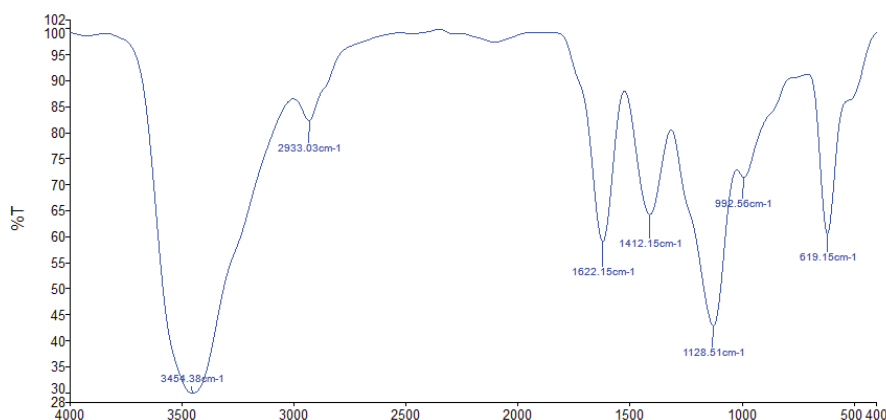Fig. 6. Sludge generated in the photo-precipitation.



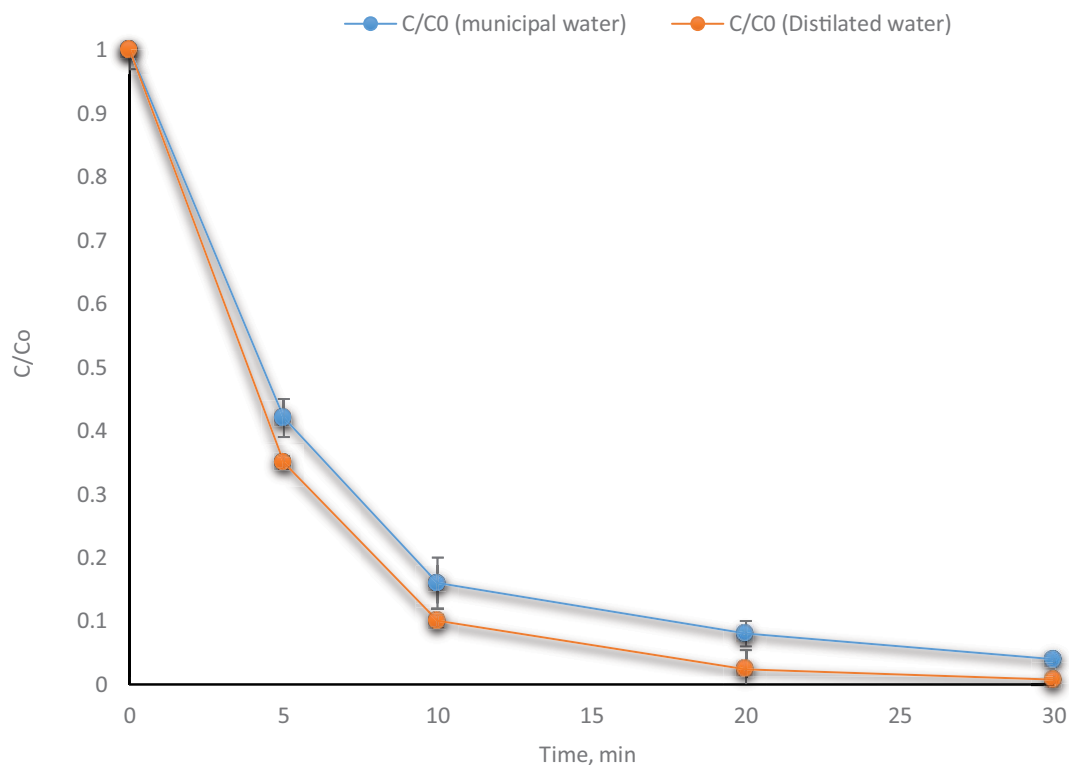Fig. 7. FTIR of different sludge created in different sulfite dose.

Fig. 8. Comparison of row water (cadmium 100 mg $L^{-1}$) and distilled sample effect in US performance (Conditions: [$Na_2SO_3$] 0.3 mM, pH 6).

in the real sample was measured through ion chromatography. A real sample of drinking water well was taken from a well which was out-of-service due to exceeding the WHO standards. The chemical parameters of the groundwater sample before and after the photo-precipitation in optimal conditions process are represented in Table 2. The presence of well water anions had a negligible effect on the performance of the cadmium photo-precipitation process and the removal efficiency. The least effect on cadmium photo-precipitation efficiency was related to sulfate and nitrate anion, which is due to the dual effect of this anions. Nitrate reacts with $e_{aq}^-$ and with sulfite radicals and does not allow the formation of complexes; meanwhile, by banding with cadmium, sulfate could help the direct removal of cadmium. Additionally, the adsorption of UV radiations through major anions and deactivation of the oxidizing and reducing species or the development of anionic radicals that are not as strong as $e_{aq}^-$ or $SO_4^{\bullet-}$ radicals cause a reduction in photodegradation. Nitrate has more acid dissociation constant ($k_a$) than other anion and thus has a greater effect [48]. The reaction between chloride, bicarbonate, nitrate, and sulfate with $e_{eq}^-$ and $SO_4^{\bullet-}$ is represented in Eqs. (32)–(39) [49]:

$$HCO_3^- + SO_4^{\bullet-} \rightarrow CO_3^{-\bullet} + H_2O \quad (32)$$

$$Cl^- + SO_4^{\bullet-} \rightarrow ClOH^{\bullet-} \quad (33)$$

$$NO_3^- + SO_4^{\bullet-} \rightarrow NO_3^\bullet + OH^- \quad (34)$$

Table 2
Chemical parameters of the real sample before and after the photo-precipitation

| Parameters | Row water | UV/$SO_3^-$ |
|---|---|---|
| pH (unit) | 8.87 | 8.01 |
| Cadmium (µg $L^{-1}$) | 196.73 | 75.1 |
| $HCO_3^-$ (mg $L^{-1}$) | 117.46 | 94.17 |
| $CO_3^{2-}$ (mg $L^{-1}$) | 47.02 | 44.87 |
| $NO_2^-$ (mg $L^{-1}$) | 17.27 | 10.65 |
| $Cl^-$ (mg $L^{-1}$) | 75.27 | 64.78 |
| $SO_4^{2-}$ (mg $L^{-1}$) | 49.91 | 126.34 |
| $HPO_4^{2-}$ (mg $L^{-1}$) | 9.68 | 8.63 |

$$SO_4^{2-} + SO_4^{\bullet-} \rightarrow 2SO_3^- + 2O^- \quad (35)$$

$$HCO_3^- + e_{aq}^- \rightarrow HCO_3^{-2} \quad (36)$$

$$Cl^- + e_{aq}^- + H^+ \rightarrow HCl \quad (37)$$

$$NO_3^- + e_{aq}^- \rightarrow \left(NO_3\right)^{\bullet 2-} \quad (38)$$

$$SO_4^{2-} + e_{aq}^- \rightarrow SO_4^{3-} \quad (39)$$

Table 3
Comparison of different catalytic methods with the present method

| Processes | Concentration of Cd | Reactive concentration | pH | Time (min) | Performance | References |
|---|---|---|---|---|---|---|
| UV/bentonite-supported Zn oxide (ZnO/BT) | 6 mg $L^{-1}$ | 4 g $L^{-1}$ | 5 | 360 | 74.8% | [40] |
| UV/TiO$_2$/Formate | 30 mg $L^{-1}$ | TiO$_2$: 10 mg $L^{-1}$; Formate: 6 mg $L^{-1}$ | 7–8 | 150 | 60% | [39] |
| CaO$_2$/ZVI | 10 mg $L^{-1}$ | 1.5 g $L^{-1}$ ZVI and 0.5 g $L^{-1}$ CaO$_2$ | 3 | 100 | 96.7% | [50] |
| UV/TiSi/formate | 100 mg $L^{-1}$ | TiSi: 1.5 g $L^{-1}$; Formate 200 mg $L^{-1}$ | 3.5 | 60 | 89% | [51] |
| UV/TiO$_2$/H$_2$O$_2$ | 10 mg $L^{-1}$ | 3 mL $L^{-1}$ H$_2$O$_2$ and 0.8 g $L^{-1}$ TiO$_2$ | 11 | 180 | 97.7% | [25] |
| Solar visible/Y-sensitized TiO$_2$ | 100 mg $L^{-1}$ | 0.503 g $L^{-1}$ | 7 | 180 | 37%–100% | [52] |
| Solar/TO/CFO | 10 mg $L^{-1}$ | 0.03 g $L^{-1}$ | 6 | 180 | 92.02% | [53] |
| Present study | 100 mg $L^{-1}$ | [Na$_2$SO$_3$] 0.1 mM | 6 | 20 | 96.41% | |

As can be seen in Table 3 for comparing different catalytic methods with the present method, the current method has many advantages. These include less time, higher efficiency, less use of reactive materials, and no need for large pH changes.

## 4. Conclusions

Herein, the removal of cadmium in a novel process, including reduction and complexion oxidation in a UV/sulfite, was investigated. The obtained information revealed that the UV/S is a very rapid process. Comparison of different catalytic methods proved that the US process needs less time, has higher efficiency and less use of reactive materials, and does not need large pH changes. This method investigated a real well sample with anions, the more effective of which were nitrate and sulfate. Nitrate reacted with $e^-_{aq}$ and sulfite radicals and did not allow the formation of complexes; on the other hand, the banding of sulfate with cadmium could result in the direct removal of cadmium.

## Acknowledgements

## References

[1] K. Rahmani, A.H. Mahvi, Biosorption of cadmium and copper ions from industrial wastewaters by waste activated sludge, Int. J. Environ. Anal. Chem., 102 (2020) 1109–1117.
[2] E. Bazrafshan, L. Mohammadi, A. Ansari-Moghaddam, A.H. Mahvi, Heavy metals removal from aqueous environments by electrocoagulation process – a systematic review, J. Environ. Health Sci. Eng., 13 (2015) 1–16, doi: 10.1186/s40201-015-0233-8.
[3] K. Naddafi, R. Nabizadeh, R. Saeedi, A.H. Mahvi, F. Vaezi, K. Yaghmaeian, A. Ghasri, S. Nazmara, Biosorption of lead(II) and cadmium(II) by protonated *Sargassum glaucescens* biomass in a continuous packed bed column, J. Hazard. Mater., 147 (2007) 785–791.
[4] A. Maleki, A.H. Mahvi, M.A. Zazouli, H. Izanloo, A.H. Barati, Aqueous cadmium removal by adsorption on barley hull and barley hull ash, Asian J. Chem., 23 (2011) 1373–1376.
[5] I. Gul, M. Manzoor, N. Hashim, G.M. Shah, S.P.T. Waani, M. Shahid, V. Antoniadis, J. Rinklebe, M. Arshad, Challenges in microbially and chelate-assisted phytoextraction of cadmium and lead – a review, Environ. Pollut., 287 (2021) 117667, doi: 10.1016/j.envpol.2021.117667.
[6] A. Mahvi, F. Gholami-borujeni, S. Nazmara, Cadmium biosorption from wastewater by Ulmus leaves and their ash, Eur. J. Sci. Res., 23 (2008) 197–203.
[7] A. Kubier, R.T. Wilkin, T. Pichler, Cadmium in soils and groundwater: a review, Appl. Geochem., 108 (2019) 104388, doi: 10.1016/j.apgeochem.2019.104388.
[8] D. Diaz, F. Ujueta, G. Mansur, G.A. Lamas, A. Navas-Acien, I.A. Arenas, Low-level cadmium exposure and atherosclerosis, Curr. Environ. Health Rep., 8 (2021) 42–53.
[9] C. Xu, Z. Weng, L. Zhang, J. Xu, M. Dahal, T.B. Basnet, A. Gu, HDL cholesterol: a potential mediator of the association between urinary cadmium concentration and cardiovascular disease risk, Ecotoxicol. Environ. Saf., 208 (2021) 111433, doi: 10.1016/j.ecoenv.2020.111433.
[10] B. Kakavandi, R.R. Kalantary, M. Farzadkia, A.H. Mahvi, A. Esrafili, A. Azari, A.R. Yari, A.B. Javid, Enhanced chromium(VI) removal using activated carbon modified by zero valent iron and silver bimetallic nanoparticles, J. Environ. Health Sci. Eng., 12 (2014) 1–10, doi: 10.1186/s40201-014-0115-5.
[11] G. Genchi, M.S. Sinicropi, G. Lauria, A. Carocci, A. Catalano, The effects of cadmium toxicity, Int. J. Environ. Res. Public Health, 17 (2020) 3782, doi: 10.3390/ijerph17113782.
[12] Y. Vasseghian, F. Almomani, E.-N. Dragoi, Health risk assessment induced by trace toxic metals in tap drinking water: condorcet principle development, Chemosphere, 286 (2021) 131821, doi: 10.1016/j.chemosphere.2021.131821.
[13] R. Aruna Devi, M. Latha, S. Velumani, G. Oza, P. Reyes-Figueroa, M. Rohini, I.G. Becerril-Juarez, J.-H. Lee, J. Yi, Synthesis and characterization of cadmium sulfide nanoparticles by chemical precipitation method, J. Nanosci. Nanotechnol., 15 (2015) 8434–8439.
[14] Sadani, T. Rasolevandi, H. Azarpira, A.H. Mahvi, M. Ghaderpoori, S.M. Mohseni, A. Atamaleki, Arsenic selective adsorption using a nanomagnetic ion imprinted polymer: optimization, equilibrium, and regeneration studies, J. Mol. Liq., 317 (2020) 114246, doi: 10.1016/j.molliq.2020.114246.
[15] M.H. Ehrampoush, M. Miria, M.H. Salmani, A.H. Mahvi, Cadmium removal from aqueous solution by green synthesis iron oxide nanoparticles with tangerine peel extract, J. Environ. Health Sci. Eng., 13 (2015) 1–7, doi: 10.1186/s40201-015-0237-4.

[16] H. Alamgholiloo, B. Hashemzadeh, N.N. Pesyan, A. Sheikhmohammadi, E. Asgari, J. Yeganeh, H. Hashemzadeh, A facile strategy for designing core-shell nanocomposite of ZIF-67/Fe$_3$O$_4$: a novel insight into ciprofloxacin removal from wastewater, Process Saf. Environ. Prot., 147 (2021) 392–404.

[17] H. Rasoulzadeh, A. Sheikhmohammadi, M. Abtahi, B. Roshan, R. Jokar, Eco-friendly rapid removal of palladium from aqueous solutions using alginate-diatomite magnano composite, J. Environ. Chem. Eng., 9 (2021) 105954, doi: 10.1016/j.jece.2021.105954.

[18] L. Rafati, A.H. Mahvi, A.R. Asgari, S.S. Hosseini, Removal of chromium(VI) from aqueous solutions using Lewatit FO36 nano ion exchange resin, Int. J. Environ. Sci. Technol., 7 (2010) 147–156.

[19] T.K. Tran, N. Kim, Q.C. Le, M.T. Nguyen, H.J. Leu, K.N.V. Thi, Electrochemical preparation and characterization of polyaniline enhanced electrodes: an application for the removal of cadmium metals in industrial wastewater, Mater. Chem. Phys., 261 (2021) 124221, doi: 10.1016/j.matchemphys.2021.124221.

[20] H.J. Mansoorian, A.H. Mahvi, A.J. Jafari, Removal of lead and zinc from battery industry wastewater using electrocoagulation process: influence of direct and alternating current by using iron and stainless steel rod electrodes, Sep. Purif. Technol., 135 (2014) 165–175.

[21] H. Liu, K. Liu, H. Fu, R. Ji, X. Qu, Sunlight mediated cadmium release from colored microplastics containing cadmium pigment in aqueous phase, Environ. Pollut., 263 (2020) 114484, doi: 10.1016/j.envpol.2020.114484.

[22] E. Asgari, B. Hashemzadeh, G. Hassani, M. Manshouri, A. Sheikhmohammadi, Y. Fakhri, Enhancement the BuP photo-catalytic degradability by UVC/ZnO through adding exogenous oxidant: mechanism, kinetic, energy consumption, J. Environ. Chem. Eng., 8 (2020) 103576, doi: 10.1016/j.jece.2019.103576.

[23] A. Figoli, C. Ursino, S. Santoro, I. Ounifi, J. Chekir, A. Hafiane, E. Ferjani, Cellulose acetate nanofiltration membranes for cadmium remediation, J. Membr. Sci. Res., 6 (2020) 226–234.

[24] E. Asgari, A. Sheikhmohammadi, H. Nourmoradi, S. Nazari, M. Aghanaghad, Degradation of ciprofloxacin by photocatalytic ozonation process under irradiation with UVA: comparative study, performance and mechanism, Process Saf. Environ. Prot., 147 (2021) 356–366.

[25] M.R. Samarghandi, J. Nouri, A.R. Mesdaghinia, A. Mahvi, S. Nasseri, F. Vaezi, Efficiency removal of phenol, lead and cadmium by means of UV/TiO$_2$/H$_2$O$_2$ processes, Int. J. Environ. Sci. Technol., 4 (2007) 19–25.

[26] T. Rasolevandi, S. Naseri, H. Azarpira, A.H. Mahvi, Photo-degradation of dexamethasone phosphate using UV/Iodide process: kinetics, intermediates, and transformation pathways, J. Mol. Liq., 295 (2019) 111703.

[27] H. Azarpira, M. Abtahi, M. Sadani, S. Rezaei, Z. Atafar, A. Bay, S.M. Mohseni, M. Sarkhosh, M. Shanbedi, H. Alidadi, Y. Fakhri, H. Keramati, V. Fanai, Photo-catalytic degradation of Trichlorophenol with UV/sulfite/ZnO process, simultaneous usage of homogeneous reductive and heterogeneous oxidative agents generator as a new approach of advanced oxidation/reduction processes (AO/RPs), J. Photochem. Photobiol., A, 374 (2019) 43–51.

[28] S. Azizi, M. Sarkhosh, A.A. Najafpoor, S.M. Mohseni, M. Mazza, M. Sadani, Degradation of codeine phosphate by simultaneous usage of e$^-_{aq}$ and $^\bullet$OH radicals in photo-redox processes: influencing factors, energy consumption, kinetics, intermediate products and degradation pathways, Optik, 243 (2021) 167415, doi: 10.1016/j.ijleo.2021.167415.

[29] M. Massoudinejad, S.M. Zarandi, M.M. Amini, S.M. Mohseni, Enhancing photo-precipitation of chromate with carboxyl radicals: kinetic, energy analysis and sludge survey, Process Saf. Environ. Prot., 134 (2020) 440–447.

[30] T. Rasolevandia, H. Azarpira, A.H. Mahvi, Modeling and optimizing chromate photo-precipitation with iodide exciting under UV irradiation, Desal. Water Treat., 195 (2020) 369–376.

[31] J. Xu, W. Ding, F. Wu, G. Mailhot, D. Zhou, K. Hanna, Rapid catalytic oxidation of arsenite to arsenate in an iron(III)/sulfite system under visible light, Appl. Catal., B, 186 (2016) 56–61.

[32] D.T.F. Kuo, D.W. Kirk, C.Q. Jia, The chemistry of aqueous S(IV)-Fe-O$_2$ system: state of the art, J. Sulfur Chem., 27 (2006) 461–530.

[33] C.-G. Lee, H. Javed, D. Zhang, J.-H. Kim, P. Westerhoff, Q. Li, P.J.J. Alvarez, Porous electrospun fibers embedding TiO$_2$ for adsorption and photocatalytic degradation of water pollutants, Environ. Sci. Technol., 52 (2018) 4285–4293.

[34] H. Gekko, K. Hashimoto, H. Kominami, Photocatalytic reduction of nitrite to dinitrogen in aqueous suspensions of metal-loaded titanium(IV) oxide in the presence of a hole scavenger: an ensemble effect of silver and palladium co-catalysts, Phys. Chem. Chem. Phys., 14 (2012) 7965–7970.

[35] U. Alam, T.A. Shah, A. Khan, M. Muneer, One-pot ultrasonic assisted sol-gel synthesis of spindle-like Nd and V codoped ZnO for efficient photocatalytic degradation of organic pollutants, Sep. Purif. Technol., 212 (2019) 427–437.

[36] L. Kong, Y. Wang, X. Hu, X. Peng, Z. Xia, J. Wang, Improving removal rate and efficiency of As(V) by sulfide from strongly acidic wastewater in a modified photochemical reactor, Environ. Technol., (2021) 1–25, doi: 10.1080/09593330.2021.1877360.

[37] L. Kong, X. Hu, X. Peng, X. Wang, Specific H$_2$S release from thiosulfate promoted by UV irradiation for removal of arsenic and heavy metals from strongly acidic wastewater, Environ. Sci. Technol., 54 (2020) 14076–14084.

[38] D. He, Y. Xiong, L. Wang, W. Sun, R. Liu, T. Yue, Arsenic(III) removal from a high-concentration arsenic(III) solution by forming ferric arsenite on red mud surface, Minerals, 10 (2020) 583, doi: 10.3390/min10070583.

[39] V.N.H. Nguyen, R. Amal, D. Beydoun, Effect of formate and methanol on photoreduction/removal of toxic cadmium ions using TiO$_2$ semiconductor as photocatalyst, Chem. Eng. Sci., 58 (2003) 4429–4439.

[40] H. Salmanvandi, P. Rezaei, Y. Tamsilian, Photoreduction and removal of cadmium ions over bentonite clay-supported zinc oxide microcubes in an aqueous solution, ACS Omega, 5 (2020) 13176–13184.

[41] J. Rinklebe, A.S. Knox, M. Paller, Eds., Trace Elements in Waterlogged Soils and Sediments, CRC Press, Florida, United States, 2016.

[42] A. Rastogi, S.R. Al-Abed, D.D. Dionysiou, Sulfate radical-based ferrous–peroxymonosulfate oxidative system for PCBs degradation in aqueous and sediment systems, Appl. Catal., B, 85 (2009) 171–179.

[43] Q. Xiao, S. Yu, L. Li, T. Wang, X. Liao, Y. Ye, An overview of advanced reduction processes for bromate removal from drinking water: reducing agents, activation methods, applications and mechanisms, J. Hazard. Mater., 324 (2017) 230–240.

[44] W. Zhang, G. Zhang, C. Liu, J. Li, T. Zheng, J. Ma, L. Wang, J. Jiang, X. Zhai, Enhanced removal of arsenite and arsenate by a multifunctional Fe-Ti-Mn composite oxide: photooxidation, oxidation and adsorption, Water Res., 147 (2018) 264–275.

[45] M.J. Lim, N.N.M. Shahri, H. Taha, A.H. Mahadi, E. Kusrini, J.W. Lim, A. Usman, Biocompatible chitin-encapsulated CdS quantum dots: fabrication and antibacterial screening, Carbohydr. Polym., 260 (2021) 117806, doi: 10.1016/j.carbpol.2021.117806.

[46] M. Khairy, H.A. Ayoub, C.E. Banks, Large-scale production of CdO/Cd(OH)$_2$ nanocomposites for non-enzyme sensing and supercapacitor applications, RSC Adv., 8 (2018) 921–930.

[47] L. Na, F. Maohong, J. Van Leeuwen, B. Saha, Y. Hongqun, C.P. Huang, Oxidation of As(III) by potassium permanganate, J. Environ. Sci., 19 (2007) 783–786.

[48] A.U. Rahmah, S. Harimurti, T. Murugesan, Experimental investigation on the effect of wastewater matrix on oxytetracycline mineralization using UV/H$_2$O$_2$ system, Int. J. Environ. Sci. Technol., 14 (2017) 1225–1233.

[49] M. Sarkhosh, M. Sadani, M. Abtahi, S.M. Mohseni, A. Sheikhmohammadi, H. Azarpira, A.A. Najafpoor, Z. Atafar, S. Rezaei, R. Alli, A. Bay, Enhancing photo-degradation of ciprofloxacin using simultaneous usage of e$^-_{aq}$ and $^\bullet$OH over UV/ZnO/I$^-$ process: efficiency, kinetics, pathways, and mechanisms, J. Hazard. Mater., 377 (2019) 418–426.

[50] C. Hou, J. Zhao, Y. Zhang, Y. Qian, J. Chen, M. Yang, J. Du, T. Chen, B. Huang, X. Zhou, Enhanced simultaneous removal

of cadmium, lead, and acetochlor in hyporheic zones with calcium peroxide coupled with zero-valent iron: mechanisms and application, Chem. Eng. J., 427 (2022) 130900, doi: 10.1016/j. cej.2021.130900.

[51] T. Mishra, J. Hait, N. Aman, R.K. Jana, S. Chakravarty, Effect of UV and visible light on photocatalytic reduction of lead and cadmium over titania based binary oxide materials, J. Colloid Interface Sci., 316 (2007) 80–84.

[52] P. Chowdhury, S. Athapaththu, A. Elkamel, A.K. Ray, Visible-solar-light-driven photo-reduction and removal of cadmium ion with Eosin Y-sensitized $TiO_2$ in aqueous solution of triethanolamine, Sep. Purif. Technol., 174 (2017) 109–115.

[53] Y. Shen, B. Xu, S. Zhu, F. Zhang, Q. Zhao, X. Li, Enhanced photocatalytic reduction of cadmium on calcium ferrite-based nanocomposites by simulated solar radiation, Mater. Lett., 211 (2018) 142–145.